

Ecosystem-scale measurements of biomass water using cosmic ray neutrons

Trenton E. Franz,^{1,2} Marek Zreda,¹ Rafael Rosolem,^{1,3} Brian K. Hornbuckle,⁴ Samantha L. Irvin,⁴ Henry Adams,⁵ Thomas E. Kolb,⁶ Chris Zweck,¹ and W. James Shuttleworth¹

Received 13 June 2013; revised 23 July 2013; accepted 25 July 2013.

[1] Accurate estimates of biomass are imperative for understanding the global carbon cycle. However, measurements of biomass and water in the biomass are difficult to obtain at a scale consistent with measurements of mass and energy transfer, ~1 km, leading to substantial uncertainty in dynamic global vegetation models. Here we use a novel cosmic ray neutron method to estimate a stoichiometric predictor of ecosystem-scale biomass and biomass water equivalent over tens of hectares. We present two experimental studies, one in a ponderosa pine forest and the other in a maize field, where neutron-derived estimates of biomass water equivalent are compared and found consistent with direct observations. Given the new hectometer scale of nondestructive observation and potential for continuous measurements, we anticipate this technique to be useful to many scientific disciplines.

Citation: Franz, T. E., M. Zreda, R. Rosolem, B. K. Hornbuckle, S. L. Irvin, H. Adams, T. E. Kolb, C. Zweck, and W. J. Shuttleworth (2013), Ecosystem-scale measurements of biomass water using cosmic ray neutrons, *Geophys. Res. Lett.*, 40, doi:10.1002/grl.50791.

1. Introduction

[2] Knowledge of biomass is critical for understanding the global carbon cycle. Observed [Korner *et al.*, 2005; Luyssaert *et al.*, 2008] and modeled carbon budgets [Purves and Pacala, 2008] differ significantly in forest ecosystems partly because it is hard to reconcile measurements of leaf-level photosynthesis with measurements of stand-scale mass and energy transfer [Ozanne *et al.*, 2003]. This disconnect in observation scales limits understanding of ecosystem function [Enquist *et al.*, 2003] and contributes substantially to uncertainty in dynamic global vegetation models (DGVM) [Purves and Pacala, 2008]. Global climate models that include DGVM exhibit improved carbon cycle simulations when accurate biomass data are included [Creutzig *et al.*, 2012].

[3] Accurate measurements of area-average biomass are difficult to obtain [Jenkins *et al.*, 2003] at a scale consistent with measurements of mass and energy transfer, ~1 km. There are three common methods for the monitoring of terrestrial carbon storage in vegetation: forest allometry measurements [Jenkins *et al.*, 2003], remote sensing of two-dimensional vegetation greenness [Hansen *et al.*, 2000], and light detection and ranging (LiDAR) techniques [Lefsky *et al.*, 2002]. In all three techniques, dry biomass is estimated through allometric relationships based on plant dimensions and then converted to carbon using stoichiometry (Figure S1 in the supporting information). However, allometric approaches are labor intensive, dependent on local species, and often biased toward smaller tree size classes with uncertainties up to 30% [Jenkins *et al.*, 2003]. While recent advances in the terrestrial and airborne LiDAR method allow the possibility of fine-scale volume and surface area information, shadowing effects from dense canopies can limit the applicability of the technique, requiring multiple vantage points and significant data processing [Loudermilk *et al.*, 2009].

[4] Here we use a novel cosmic ray neutron method [Zreda *et al.*, 2008] to estimate average biomass water equivalent, and thus biomass through stoichiometry, over an area of tens of hectares [Desilets and Zreda, 2013]. The method provides an integrated measure of both fixed biological hydrogen in the plant tissue and biological water contained in the plant xylem and other tissues, the sum of which we call biomass water equivalent (BWE; Figure S1). Although neutron intensity depends on all hydrogen pools near the ground [Zreda *et al.*, 2012], we are able to isolate the biomass water signal using measurements of neutron intensity, soil water content, soil mineral water, and atmospheric water vapor [Franz *et al.*, 2013]. In this work we present two experimental studies in forest and agricultural settings that give snapshots in time of neutron-derived estimates of biomass water that are consistent with direct observations. Given the spatial scale of observations and potential for continuous estimates of biomass water equivalent, this method could fill a critical observation gap in monitoring ecosystem-scale carbon and water dynamics.

2. Cosmic Ray Neutron Method

2.1. Background of Cosmic Rays on Earth and Neutron Detection

[5] Victor Hess received the Nobel Prize in Physics (1936) for his discovery of cosmic rays in 1912. During the midtwentieth century, scientists found, through both theoretical and experimental work, that the intensity of low-energy cosmic ray neutrons depends on the chemical composition

Additional supporting information may be found in the online version of this article.

¹University of Arizona, Department of Hydrology and Water Resources, Tucson, Arizona, USA.

²Now at the University of Nebraska-Lincoln, School of Natural Resources.

³Now at the University of Bristol, Department of Civil Engineering.

⁴Iowa State University, Department of Agronomy, Ames, Iowa, USA.

⁵Los Alamos National Laboratory, Los Alamos, New Mexico, USA.

⁶Northern Arizona University, School of Forestry, Flagstaff, Arizona, USA.

Corresponding author: T. E. Franz, University of Arizona, 1133 E. James E. Rogers Way, Rm. 122, Tucson, AZ 85721, USA. (tfranz@email.arizona.edu)

of the material, in particular the medium's hydrogen content due to its high moderation power (as summarized with references in *Zreda et al.* [2012]). Fast neutrons (~ 1 MeV), a tertiary cosmic ray flux created by high-energy secondary cosmic ray neutrons, exist in a well-mixed reservoir comprising soil and air [*Zreda et al.*, 2012]. During the moderation process, fast neutrons can mix at the scale of hundreds of meters in air and tens of centimeters in soil [*Desilets*, 2011].

[6] The principles of neutron detection with proportional counters are well established [*Knoll*, 2000]. Here we use the moderated or fast neutron detector implemented in the COsmic-ray Soil Moisture Observing System (COSMOS) [*Zreda et al.*, 2012]. The fast neutron detector is shielded by 2.5 cm of plastic, making it most sensitive to neutrons between 1 and 1000 eV [*Desilets*, 2011]. We note from neutron transport modeling that the relationship between average hydrogen content and neutron flux is nearly identical over these energy ranges (T. E. Franz, unpublished data, 2013).

2.2. Estimation of Biomass Water Equivalent Using Fast Neutron Intensity

[7] While the fast neutron detector used here was originally designed to measure soil water dynamics in the near surface over large horizontal areas (~ 28 ha, a circle with radius of ~ 300 m at sea level in dry air [*Desilets and Zreda*, 2013], vertical depths of ~ 10 cm in wet soil and ~ 70 cm in dry soil [*Zreda et al.*, 2008]), it is sensitive to all hydrogen inside its measurement volume [*Zreda et al.*, 2012]. By independently quantifying soil moisture (and other nonbiomass hydrogen pools) with direct sampling, we are able to isolate the biomass water signal component in the fast neutron intensity measurements following the framework outlined in [*Franz et al.*, 2013]. Because soil water is typically the largest pool of hydrogen present in the near surface, its uncertainty will control the measurement precision of the biomass hydrogen pool. Despite the large horizontal and vertical heterogeneity, we found from extensive soil moisture field sampling at numerous COSMOS sites (108 total samples collected at each site at six depths, 0–30 cm every 5 cm, and 18 horizontal locations, 0–360° every 60°, and radii of 25, 75, and 200 m) that the standard error of the mean soil moisture as a function of mean soil moisture has a parabolic shape with a maximum value of $0.008 \text{ m}^3/\text{m}^3$ equivalent to 2.4 mm of water or $2.4 \text{ kg}/\text{m}^2$ at a soil water content of $0.275 \text{ m}^3/\text{m}^3$ (Figure S2).

[8] In order to isolate the biomass water signal from the convoluted fast neutron intensity measurements, we need to make several assumptions and simplifications about the instrument support volume, instrument sensitivity, estimation of various hydrogen pools inside the support volume through direct sampling, and distribution of hydrogen pools within the support volume. Because the various hydrogen pools can be aggregated in a thin layer (i.e., soil pore water, soil mineral water, and vegetation) or dispersed across the entire support volume (i.e., water vapor and forests), our framework either directly accounts for the mass of the hydrogen pool or removes its signal from the convoluted signal using derived relationships from neutron transport simulations [*Franz et al.*, 2013; *Zreda et al.*, 2012].

[9] Here we assume that the instrument support volume (86% cumulative sensitivity) is a hemisphere above the surface with a constant radius of 300 m as defined by previous work [*Desilets and Zreda*, 2013; *Zreda et al.*, 2008]. We note

that *Desilets and Zreda* [2013] found that the support radius is reduced by 20 m per additional 10 g of water per kilogram of air but does increase with elevation above sea level. In order to remove the water vapor component from the fast neutron intensity measurements, we use measurements of surface air temperature, air pressure, and relative humidity to determine the absolute humidity [*Rosolem et al.*, 2013]. *Rosolem et al.* [2013] found the neutron correction factor as

$$\text{CWV} = 1 + 0.0054(\rho_v^0 - \rho_v^{\text{ref}}) \quad (1)$$

where CWV is the scaling factor for temporal changes in cosmic ray intensity as a function of changes in atmospheric water vapor, ρ_v^0 (g m^{-3}) is the absolute humidity at the surface, and ρ_v^{ref} (g m^{-3}) is the absolute humidity at the surface at a reference condition (here we use dry air, $\rho_v^{\text{ref}} = 0$).

[10] Because vegetation in forests may be distributed in clumps across the support volume, we introduce an additional correction factor relating the efficiency of neutron moderation from discrete objects versus an equivalent layer of water on the surface (CBWE). Neutron transport simulations indicate that the equivalent layer efficiency factor depends on both the total volume and surface area of tree trunks (Figure S3). Therefore, a priori information is needed about the size and distribution of trunks inside the measurement volume. We note that the support radius and depth will be only slightly reduced by the presence of aboveground biomass given the large open space for neutrons to travel unimpeded. In order to correct for dispersed hydrogen pools above the surface, we define the dry atmosphere neutron counting rate N (counts per hour, cph) as

$$N = N_{L2} \times \text{CWV} \times \text{CBWE} \quad (2)$$

where N_{L2} is the level 2 neutron counting rate (<http://cosmos.hwr.arizona.edu/>) previously corrected for variations in incoming high-energy particles and absolute pressure deviations [*Zreda et al.*, 2012].

[11] Below the surface, we assume that the support volume is a cylinder with a fixed radius of 300 m and a depth that varies with surface water, soil pore water, mineral water, and bulk density. Assuming no surface water and uniform distributions of soil pore water, mineral water, and bulk density, *Franz et al.* [2012] found the effective sensing depth z^* (cm) to be approximated by the following equation [*Franz et al.*, 2012]:

$$z^* = \frac{5.8}{\frac{\rho_{bd}}{\rho_w}(\tau + \text{SOC}) + \theta + 0.0829} \quad (3)$$

where 5.8 (cm) represents the 86% cumulative sensitivity depth of low-energy neutrons in liquid water; 0.0829 is controlled by the nuclear cross sections of SiO_2 ; ρ_{bd} is the dry bulk density of soil (g cm^{-3}); ρ_w is the density of liquid water assumed to be $1 \text{ (g cm}^{-3}\text{)}$; τ is the weight fraction of lattice water in the mineral grains and bound water, defined as the amount of water released at 1000°C preceded by drying at 105°C (gram of water per gram of dry minerals); and SOC is the soil organic carbon (gram of water per gram of dry minerals, estimated from stoichiometry using measurements of total soil carbon, TC, and soil CO_2 , $\text{SOC} = \text{TC} - \frac{12}{44}\text{CO}_2$). Here measurements of lattice water, total soil carbon, and soil CO_2 were made on an ~ 100 g composite sample (subsampling from the 108 soil moisture samples) collected at the study site and analyzed at Actlabs Inc. of Ontario, Canada.

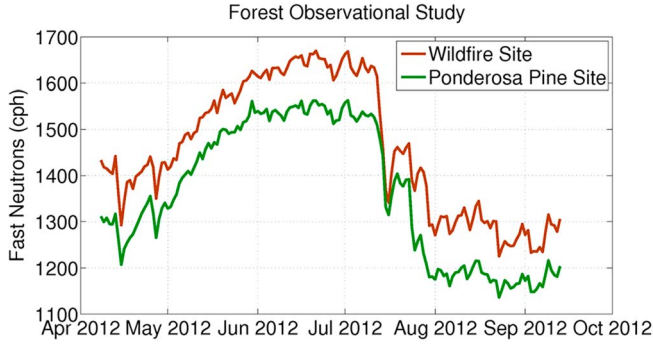


Figure 1. Time series of daily fast neutron counts at the study sites near Flagstaff, AZ, USA. One cosmic ray neutron probe was placed in a burned area, wildfire (brown line), and the other 3 km away in an intact ponderosa pine forest (green line). The sharp decreases in neutron counts are due to rainfall, and the slow increases in neutrons counts are due to loss of soil water to evapotranspiration and deep infiltration. Because of the additional hydrogen in the intact ponderosa pine forest, the neutron counts are consistently lower at that site throughout the year. Note that the daily averaged Poisson counting rate uncertainty is between 7 and 9 cph and that there is an inverse relationship between neutron counts and total hydrogen present because of hydrogen’s high efficiency in removing neutrons.

[12] With the estimates of sensor support volume, we can compute the mass and molar mass of each element in the system. We assume that the atmosphere is composed of only nitrogen (79% by mass) and oxygen (21% by mass) and follows a standard lapse rate. We further assume that the subsurface is composed of solid grains (pure quartz, SiO_2 , lattice water, and SOC water equivalent) and soil pore water. Here we assume that the wet aboveground biomass, AGB (kg/m^2), is composed of only water (50% by mass) and cellulose ($\text{C}_6\text{H}_{10}\text{O}_5$, 50% by mass) but note that this is dependent on plant species and time and should be quantified directly. With the estimates of volume, mass, and chemical composition, we can calculate the hydrogen molar fraction, hmf (mol mol^{-1}), in the cosmic ray probe support volume as

$$\text{hmf} = \frac{\sum H_i}{\sum A_i} = \frac{H_r + H_{\text{SOC}} + H_\theta + H_{\text{AGB}}}{\text{NO} + \text{SiO}_2 + \text{H}_2\text{O}_r + \text{H}_2\text{O}_{\text{SOC}} + \text{H}_2\text{O}_\theta + \text{C}_6\text{H}_{10}\text{O}_5 + \text{H}_2\text{O}_{\text{AGB}}} \quad (4)$$

where $\sum H_i$ is the sum of hydrogen moles from lattice water H_r , soil organic carbon water equivalent H_{SOC} , pore water H_θ , and vegetation H_{AGB} inside the support volume, and $\sum A_i$ is the sum of all moles from air NO, soil SiO_2 , lattice water H_2O_r , soil organic carbon water equivalent $\text{H}_2\text{O}_{\text{SOC}}$, pore water $\text{H}_2\text{O}_\theta$, and aboveground biomass $\text{C}_6\text{H}_{10}\text{O}_5 + \text{H}_2\text{O}_{\text{AGB}}$ inside the support volume.

[13] Using neutron transport modeling simulations of various soil chemistries, Franz *et al.* [2013] derived a single relationship between hmf and relative neutron counts:

$$\frac{N}{N_s} = 4.486 \exp(-48.1 \times \text{hmf}) + 4.195 \exp(-6.181 \times \text{hmf}) \quad (5)$$

where N_s represents the site- and instrument-specific fast neutron count rate at saturation (i.e., over liquid water, where the count rates approach a constant value). We note that in this work, we used a single known value of hmf and the

corresponding N to specify the free parameter N_s in order to minimize site, instrument, and sampling uncertainties. By measuring (either at one snapshot in time or continuously) fast neutron intensity, water vapor, soil pore water, and soil mineral water, estimates of BWE ($=0.556 \times \text{C}_6\text{H}_{10}\text{O}_5 + \text{H}_2\text{O}_{\text{ABG}}$) can be calculated using equations (1) to (5).

3. Biomass and Biological Water Content

3.1. Estimates of Forest Biomass

[14] To evaluate forest biomass and BWE, a semiarid site near Flagstaff, AZ, USA was instrumented with two identical neutron probes (CRS-1000/B), placed 3 km apart: one in a ponderosa pine forest ($35^\circ 26' 19''\text{N}$, $111^\circ 48' 13''\text{W}$) and the other in an area burned by wildfire in 1996 ($35^\circ 26' 44''\text{N}$, $111^\circ 46' 19''\text{W}$) [Dore *et al.*, 2010]. We note that the probes were tested side by side over an 18 h period and were found statistically identical. The measured fast neutron count rate at the ponderosa pine site was consistently ~ 100 cph lower than that at the wildfire site (Figure 1). This difference can be attributed to more efficient removal of fast neutrons by the additional hydrogen present in the aboveground biomass at the forest site (Table S1). Measurements at the burned site and surrounding ponderosa pine forest give similar belowground carbon pools ($\sim 7 \text{ kg C}/\text{m}^2$ in Dore *et al.* [2010] and Table S1). Stem density measurements [Dore *et al.*, 2010, Figure 1], carbon pool estimates [Dore *et al.*, 2010, Table 4], and allometric relationships of the stem density measurements [Jenkins *et al.*, 2003] give the aboveground wet ponderosa pine biomass between 16 and $31 \text{ kg}/\text{m}^2$. By solving equations (1) to (5) using independent measurements of water in soil minerals, soil pore water, atmospheric water

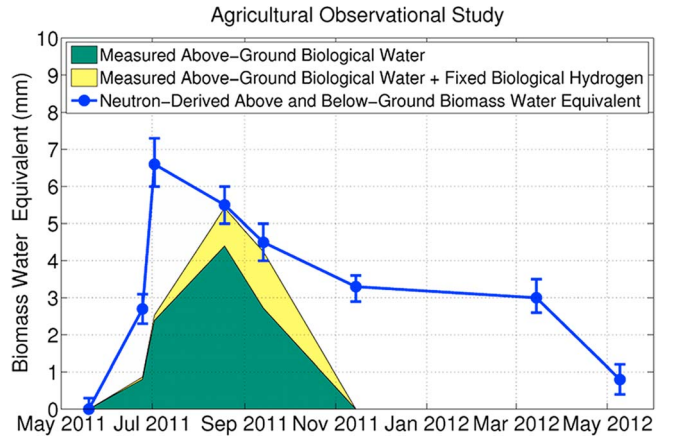


Figure 2. Measured aboveground biological water (green area), sum of measured aboveground biological water and fixed biological hydrogen (yellow + green area), and neutron-derived aboveground and belowground biomass water equivalent (blue line) at the Iowa validation site for one rotation of maize. The differences in the neutron-derived BWE values are likely due to the presence of roots and residue (dead plant material) that is left on the soil surface after harvest. Soil tillage between the March and May 2012 measurements promoted the decomposition of the root and residue BWE. Note that the standard error of the mean was estimated from the uncertainty in the soil pore water samples (Table S2) and that the ratio of the green to yellow + green area gives the fraction of biological to total water inside the maize.

vapor, and fast neutron intensity, we found that the neutron-derived BWE of 26.9 ± 1 mm at the ponderosa pine site was within 1 standard error of 22.5 ± 4 , 34.2 ± 10 , and 32.3 ± 11 mm obtained using three different independent allometric methods (Figure S4 and Tables S1–S3).

3.2. Estimates of Maize Biomass

[15] The second study was conducted at the Iowa validation site (IVS; $41^{\circ}59'0''\text{N}$, $93^{\circ}41'1''\text{W}$) where a neutron detector (CRS-1000) was placed in the agricultural field in September 2010. The field is $1 \text{ km} \times 1 \text{ km}$ with yearly rotation between soy (even years) and maize (odd years). Estimates of water in soil minerals, soil pore water, atmospheric water vapor, and aboveground fixed hydrogen and biological water were made eight times between May 2011 and May 2012 (Table S1). These measurements were used to compute the neutron-derived BWE at various stages of maize development throughout the season (Figure 2). In early growth stages (May to June), the maize comprises over 90% water when rapidly growing both above and below ground. During flowering, fruit development, and ripening (July to August), the aboveground biological water dropped to below 70%. Comparisons of observed aboveground fixed biological hydrogen and biological water with neutron-derived BWE show similar overall behavior over the year but with several key differences (Figure 2). Because of the hydrogen in roots, the neutron-derived BWE was higher than the aboveground observations and exhibits different behaviors during the most active period of maize growth (July 2011). After harvesting (September 2011), the neutron-derived BWE remained constant over the winter months as the rootstock and dead plant material (residue) remain in the soil and on the soil surface. After soil temperatures increase and tillage occurs (May 2012), the neutron-derived BWE returned to near zero (premaize conditions) because of the (1) corresponding decrease in aboveground storage in residue, (2) decomposition of root mass and residue, and (3) mechanical vertical mixing of root mass and residue during soil tillage below the probe measurement depth of ~ 20 – 30 cm.

4. Discussion and Limitations of the Study

[16] These two field experiments demonstrate that measurements of cosmic ray neutrons can provide precise and accurate estimates of area-average BWE for a ponderosa pine forest and a maize field. But there are a few caveats that should be kept in mind when using neutrons to estimate BWE.

[17] First, because the water in the soil pore space is the largest pool of hydrogen (between 6 and 9 cm of water in the top 30 cm of soil at these two sites) and most variable in time, the precision of neutron-derived BWE estimates is primarily controlled by the standard error of the mean soil moisture measurement (Figure S2). Using the 108-sample COSMOS soil moisture protocol, we found that the standard error of the mean soil moisture had a maximum value of around $0.008 \text{ m}^3/\text{m}^3$ or 2.4 mm of water or $2.4 \text{ kg}/\text{m}^2$, thus defining the maximum precision of the technique given no other sources of uncertainty. While the 108 samples can usually be collected over several hours at a site, the methodology is still labor intensive in order to achieve the desired level of precision to be consistent with species-specific allometric relationships [Jenkins *et al.*, 2003].

[18] Second, integrated water vapor in the layer of air between the land surface and ~ 300 m above the surface may change seasonally by up to 1 cm of liquid water [Rosolem *et al.*, 2013], which is about the same magnitude as the seasonal variations in maize and total aboveground biomass at the ponderosa pine forest. Therefore, measurements of atmospheric water vapor are critical to detect the BWE signal from the integrated fast neutron intensity data.

[19] Third, the framework used to deconvolve the fast neutron intensity signal summarized in equations (1) to (5) [Franz *et al.*, 2013] required an efficiency factor (Figure S3) to convert the dispersed hydrogen of trees into an equivalent layer. Future observational and theoretical work should focus on validating these efficiency factors in various forests.

[20] Fourth, the belowground biomass and crop residue were found to be two important pools that we did not explicitly quantify in the maize IVS study. While our results demonstrate that these pools could be quantified with the cosmic ray neutron methodology, future studies can improve on these estimates. We also note that by comparing the neutron-derived BWE with observed AGB in early maize growth stages, the belowground component was significantly higher (~ 2 to 3) than published root to shoot values (~ 1) [Anderson, 1988], but these values should be validated in future work. Given the importance of root density for water uptake, measurements of root mass at large scales may be useful in helping parameterize and calibrate large-scale crop models. In addition, the slow decay or long turnover time of plant residue is a potentially huge and poorly known carbon source [Schmidt *et al.*, 2011]. The neutron-derived measurements of water equivalence presented here suggest that this technique may be useful in estimating large-scale turnover times of soil organic hydrocarbons in the near surface.

[21] **Acknowledgments.** This research and the COSMOS project are supported by the U.S. National Science Foundation under grant AGS-0838491. The fundamental work on the systematics of low-energy neutrons at the earth's surface was funded by the U.S. National Science Foundation under grants EAR-01-26241, EAR-0345440, and EAR-0636110.

[22] The Editor thanks Heye Bogen for assistance in evaluating this paper.

References

- Anderson, E. L. (1988), Tillage and N fertilization effects on maize root growth and root:shoot ratio, *Plant Soil*, *108*, 245–251.
- Creutzig, F., A. Popp, R. Plevin, G. Luderer, J. Minx, and O. Edenhofer (2012), Reconciling top-down and bottom-up modelling on future bioenergy deployment, *Nat. Clim. Chang.*, *2*(5), 320–327, doi:10.1038/nclimate1416.
- Desilets, D. (2011), Sandia Report: SAND2011-1101, Radius of influence for a cosmic-ray soil moisture probe: Theory and Monte Carlo simulations, Sandia National Laboratories, Albuquerque, New Mexico 87185 and Livermore, California 94550.
- Desilets, D., and M. Zreda (2013), Footprint diameter for a cosmic-ray soil moisture probe: Theory and Monte Carlo simulations, *Water Resour. Res.*, *49*, 3566–3575, doi:10.1002/wrcr.20187.
- Dore, S., T. E. Kolb, M. Montes-Helu, S. E. Eckert, B. W. Sullivan, B. A. Hungate, J. P. Kaye, S. C. Hart, G. W. Koch, and A. Finkral (2010), Carbon and water fluxes from ponderosa pine forests disturbed by wildfire and thinning, *Ecol. Appl.*, *20*(3), 663–683, doi:10.1890/09-0934.1.
- Enquist, B. J., E. P. Economo, T. E. Huxman, A. P. Allen, D. D. Ignace, and J. F. Gillooly (2003), Scaling metabolism from organisms to ecosystems, *Nature*, *423*(6940), 639–642, doi:10.1038/nature01671.
- Franz, T. E., M. Zreda, P. A. Ferre, R. Rosolem, C. Zweck, S. Stillman, X. Zeng, and W. J. Shuttleworth (2012), Measurement depth of the cosmic-ray soil moisture probe affected by hydrogen from various sources, *Water Resour. Res.*, *48*, W08515, doi:10.1029/2012WR011871.

- Franz, T. E., M. Zreda, R. Rosolem, and P. A. Ferre (2013), A universal calibration function for determination of soil moisture with cosmic-ray neutrons, *Hydrol. Earth Syst. Sci.*, *17*, 453–460, doi:10.5194/hess-17-453-2013.
- Hansen, M. C., R. S. Defries, J. R. G. Townshend, and R. Sohlberg (2000), Global land cover classification at 1km spatial resolution using a classification tree approach, *Int. J. Remote Sens.*, *21*(6–7), 1331–1364.
- Jenkins, J. C., D. C. Chojnacky, L. S. Heath, and R. A. Birdsey (2003), National-scale biomass estimators for United States tree species, *For. Sci.*, *49*(1), 12–35.
- Knoll, G. F. (2000), *Radiation Detection and Measurement*, John Wiley & Sons, Inc., Hoboken, NJ.
- Komer, C., R. Asshoff, O. Bignucolo, S. Hattenschwiler, S. G. Keel, S. Pelaez-Riedl, S. Pepin, R. T. W. Siegwolf, and G. Zotz (2005), Carbon flux and growth in mature deciduous forest trees exposed to elevated CO₂, *Science*, *309*(5739), 1360–1362, doi:10.1126/science.1113977.
- Lefsky, M. A., W. B. Cohen, G. G. Parker, and D. J. Harding (2002), Lidar remote sensing for ecosystem studies, *BioScience*, *52*(1), 19–30, doi:10.1641/0006-3568(2002)052[0019:lrsfes]2.0.co;2.
- Loudermilk, E. L., J. K. Hiers, J. J. O'Brien, R. J. Mitchell, A. Singhanian, J. C. Fernandez, W. P. Cropper, and K. C. Slatton (2009), Ground-based LIDAR: A novel approach to quantify fine-scale fuelbed characteristics, *Int. J. Wildland Fire*, *18*(6), 676–685, doi:10.1071/wf07138.
- Luyssaert, S., E. D. Schulze, A. Borer, A. Knohl, D. Hessenmoller, B. E. Law, P. Ciais, and J. Grace (2008), Old-growth forests as global carbon sinks, *Nature*, *455*(7210), 213–215, doi:10.1038/nature07276.
- Ozanne, C. M. P., et al. (2003), Biodiversity meets the atmosphere: A global view of forest canopies, *Science*, *301*(5630), 183–186, doi:10.1126/science.1084507.
- Purves, D., and S. Pacala (2008), Predictive models of forest dynamics, *Science*, *320*(5882), 1452–1453, doi:10.1126/science.1155359.
- Rosolem, R., W. J. Shuttleworth, M. Zreda, T. E. Franz, X. Zeng, and S. A. Kurc (2013), The effect of atmospheric water vapor on the cosmic-ray soil moisture signal, *J. Hydrometeorol.*, doi:10.1175/JHM-D-12-0120.1.
- Schmidt, M. W. I., et al. (2011), Persistence of soil organic matter as an ecosystem property, *Nature*, *478*(7367), 49–56, doi:10.1038/nature10386.
- Zreda, M., D. Desilets, T. P. A. Ferre, and R. L. Scott (2008), Measuring soil moisture content non-invasively at intermediate spatial scale using cosmic-ray neutrons, *Geophys. Res. Lett.*, *35*, L21402, doi:10.1029/2008gl035655.
- Zreda, M., W. J. Shuttleworth, X. Xeng, C. Zweck, D. Desilets, T. E. Franz, and R. Rosolem (2012), COSMOS: The COsmic-ray Soil Moisture Observing System, *Hydrol. Earth Syst. Sci.*, *16*, 4079–4099, doi:10.5194/hess-16-1-2012.